ChemComm



View Article Online

COMMUNICATION



Cite this: Chem. Commun., 2015, 51, 13102

Received 2nd June 2015, Accepted 5th July 2015

DOI: 10.1039/c5cc04510j

www.rsc.org/chemcomm

MFI zeolite nanosheets with post-synthetic Ti grafting for catalytic epoxidation of bulky olefins using H_2O_2 [†]

Jaeheon Kim,^{ab} Joonsoo Chun^{ab} and Ryong Ryoo*^{ab}

The external surfaces of the surfactant-directed, 2.5 nm MFI zeolite nanosheets were grafted with Ti using titanium(IV) butoxide. The Ti/MFI nanosheets exhibited a remarkable catalytic performance for epoxidation of bulky olefins using H_2O_2 as an oxidant, in comparison to the mesoporous silicas with amorphous frameworks.

Epoxides are some of the most valuable compounds as intermediates in the chemical industry.¹ For the production of epoxides, nanoporous titanosilicates have been extensively studied as heterogeneous catalysts using peroxides.² In particular, zeolitic microporous crystalline materials (e.g., TS-1, TS-2, Ti-MWW, etc.) have attracted much attention as environmentally benign catalysts due to their ability to catalyze epoxidations using H₂O₂.²⁻⁵ Characterization of the Ti species using EXAFS, XANES and diffusereflectance ultraviolet (DR-UV) spectroscopy has indicated that the high catalytic performance was due to the presence of Ti atoms with a tetrahedral coordination within the crystalline frameworks.⁶⁻¹⁰ When applied for bulky molecular epoxidations, however, the zeolitic titanosilicates exhibited poor catalytic conversions due to the steric constraint of the micropores. Considerable efforts were devoted to the synthesis of titanosilicate molecular sieves with mesopores that could facilitate facile diffusion of bulky reactants and products (e.g., TiMCM-41, TiSBA-15, etc.).¹¹⁻¹⁸ The titanosilicates with large pores and high external surface areas were very active and selective when organic peroxides were used as oxidants. When H₂O₂ was an oxidant, however, the

amorphous titanosilicates exhibited poor catalytic performances. In addition, Ti leaching was a problem under the catalytic reaction conditions using aqueous solutions of H₂O₂.¹⁷

To resolve the problem of the amorphous titanosilicates, many studies have examined the synthesis of mesoporous materials built with crystalline zeolitic frameworks or microporous titanosilicate zeolite analogues having the morphology of nanosheets.¹⁹⁻²⁴ The zeolitic titanosilicate nanosheets exhibited a good catalytic performance for epoxidation of bulky olefins using H_2O_2 . However, the direct synthesis of the zeolitic titanosilicates required the completely hydroxide form of zeolite structure-directing agents under strictly Na-free synthesis conditions.²¹⁻²³ To circumvent the strict and expensive synthesis requirements, Corma et al. studied post-synthetic grafting of Ti onto the surface of delaminated MWW zeolites.¹⁹ Ti grafting was effective for epoxidations using t-butyl hydroperoxide (TBHP), but not with H₂O₂. In later studies, a method to obtain H2O2-using titanosilicate catalysts was developed by the substitution of B by Ti in a borosilicate zeolite. This postsynthetic B-to-Ti substitution method was reported to be effective for bulk titanosilicate zeolites.^{24–27} Very recently, Ouyang et al. performed the B-to-Ti substitution using delaminated MWW nanosheets, but their epoxidation report was limited to the use of TBHP.²⁴ Clearly, carrying out epoxidations using H₂O₂ remained a challenge.

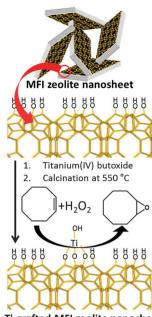
We undertook the present work to discover a facile postsynthetic route to titanosilicate zeolite nanosheets or mesoporous zeolites that could exhibit high catalytic performance for bulky molecular epoxidations using H_2O_2 . We tested various Ti incorporation methods for the surfactant-directed MFI zeolite nanosheets, such as the direct synthesis in titanosilicates, postsynthetic grafting of Ti using TBOT, and B-to-Ti substitution (the details of catalyst preparation, characterization and epoxidation reactions are given in the ESI†). Beyond our expectations, the most effective method was the post-synthetic grafting using TBOT. The MFI zeolite nanosheets prepared in this manner exhibited a high catalytic performance for bulky olefin epoxidations, even when H_2O_2 was the oxidant. Herein, we report the

^a Department of Chemistry, KAIST, Daejeon 305-701, Korea.

E-mail: rryoo@kaist.ac.kr

^b Center for Nanomaterials and Chemical Reactions, Institute for Basic Science (IBS), Daejeon 305-701, Korea

 $[\]dagger$ Electronic supplementary information (ESI) available: Synthesis procedure for MFI zeolite nanosheets, D-TiM41, G-TiM41, D-TiNS, and TS-1; preparation and catalytic data of the Ti-containing MFI zeolite nanosheets by the B-to-Ti substitution method; additional FT-IR spectrum data of MFI zeolite nanosheets before and after Ti grafting; procedures and catalytic data of post treatment with silylating agents or NH₄F; N₂ sorption, XRD, and DR-UV results of TS-1, D-TiM41, G-TiM41, D-TiNS, and MFI zeolite nanosheets prepared by the B-to-Ti substitution method; the TEM image of MFI zeolite nanosheets; the SEM image of TS-1. See DOI: 10.1039/c5cc04510j



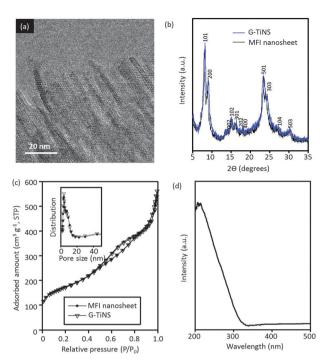
Ti-grafted MFI zeolite nanosheet

 $\label{eq:scheme1} \begin{array}{l} \mbox{Scheme1} & \mbox{Scheme1}$

catalyst preparation, characterization, and epoxidation of bulky molecular olefins with particular focus on the post-synthetic grafting of Ti.

Our Ti grafting was performed as shown in Scheme 1. In brief, a sample of MFI zeolite nanosheets possessing intersheet mesopores was synthesized in a high-purity siliceous form, following the hydrothermal synthesis procedure using $[C_{18}H_{37}-N^+(CH_3)_2-(CH_2)_6-N^+(CH_3)_2-C_6H_7][Br^-]_2$.²⁸ The MFI nanosheets were calcined at 550 °C. This zeolite was slurried in a TBOT solution dissolved in anhydrous 1-butanol (SiO₂/TBOT/butanol = 100/1/327 in mole ratio), for 1 h at 60 °C with magnetic stirring. After the 1-butanol in the slurry was completely evaporated on a warm hotplate, the zeolite was calcined again at 550 °C to remove organics. The calcined sample was characterized and tested as a catalyst for epoxidation of olefins using H₂O₂. The details of the measurements and experimental procedure are described in the ESI.† Herein, the Ti-grafted MFI nanosheet is denoted by 'G-TiNS' for brevity.

Fig. 1 shows the characterization results for the G-TiNS zeolite. Notably, in comparison to the parent zeolite nanosheets, the G-TiNS sample exhibited the same transmission electron micrographs (TEM), X-ray powder diffraction (XRD) patterns, and N_2 adsorption isotherms (Fig. 1a–c). The results indicated that the mesoporous texture and zeolitic microporous crystalline structure were not changed by the Ti-grafting process. The TEM images were consistent with unilamellar MFI zeolite nanosheets of 2.5 nm thickness along the crystal *b*-axis (Fig. 1a).²⁸ The XRD pattern exhibited Bragg diffraction peaks characteristic of the ultrathin MFI zeolite (Fig. 1b). None of the (0*k*0) reflections were observed in the XRD pattern, according to the 2-dimensional sheet-like morphology. The zeolite nanosheets retained a large volume of intersheet mesopores, without coalescence upon calcination.



View Article Online

ChemComm

Fig. 1 (a) The TEM image, (b) XRD pattern, (c) N_2 sorption isotherm (inset of c) pore size distribution, and (d) DR-UV spectrum of the G-TiNS sample. Panels (b) and (c) include the results of the siliceous MFI zeolite nanosheets before Ti-grafting, in comparison to G-TiNS.

The mesopore diameters were somewhat broadly distributed over 3-15 nm (Fig. 1c). Nevertheless, due to the microporous framework with a highly mesoporous morphology, the G-TiNS zeolite showed a large total pore volume of 0.71 $\text{cm}^3 \text{ g}^{-1}$ and a high Brunauer-Emmett-Teller (BET) surface area of 609 m² g⁻¹ (see Table 1). Fig. 1d shows the DR-UV spectrum, which was measured to evaluate the electronic state of the Ti species in G-TiNS. The DR-UV spectrum exhibited a peak centered at 220 nm (Fig. 1d). This peak could be assigned to isolated Ti sites with a tetrahedral coordination. A shoulder appeared in the 260-300 nm region in the UV absorption peak, but the intensity of this peak corresponding to the undesirable polymeric TiO₂ species was very low. Other porous titanosilicate samples, such as D-TiM41, G-TiM41, D-TiNS, and TS-1, were also investigated using DR-UV. The D-TiM41 sample was a mesoporous MCM-41 titanosilicate sample incorporating Ti

Table 1	Physicochemical properties of titanosilicate samples								
Catalyst	Ti-incorporation	Si/Ti ^a	${S_{\mathrm{BET}}}^b_{\left(\mathrm{m}^2\mathrm{g}^{-1} ight)}$	${{S_{\mathrm{ext}}}^{c} \choose {\mathrm{m}^{2} \mathrm{g}^{-1}}}$	${ S_{\mathrm{meso}} \atop \left(\mathrm{m}^2 \mathrm{g}^{-1} ight) }^{d}$	$\begin{matrix} V_{\rm t}^{e} \\ ({\rm cm}^3~{\rm g}^{-1}) \end{matrix}$			
	Direct synthesis		861	n.d. ^f	854	0.72			
	Grafting	97	970	n.d.	970	0.77			
D-TiNS	Direct synthesis	54	578	395	n.d.	0.65			
G-TiNS	Grafting	98	609	448	n.d.	0.71			
TS-1	Direct synthesis	49	380	50	n.d.	0.20			

^{*a*} Si/Ti mole ratio measured by inductively coupled plasma atomic emission spectroscopy. ^{*b*} Total surface area derived by BET methods. ^{*c*} External surface area calculated using *t*-plot methods. ^{*d*} S_{BET} – microporous surface area calculated using *t*-plot methods. ^{*e*} Total pore volume at $P/P_0 = 0.97$. ^{*f*} Not determined.

 Table 2
 Catalytic performance of titanosilicate samples for epoxidation of olefins^a

Olefins	Catalyst	$\operatorname{Conv.}^{b}(\%)$	Sel. ^c (%)	TON ^d	E^{e} (%)
Cyclootene	D-TiM41	6.1	81	18	75
	G-TiM41	4.3	83	24	77
	D-TiNS	10.1	97	31	95
	G-TiNS	9.7	95	54	93
	TS-1	0.7	$n.d.^{f}$	n.d.	n.d.
Cycloodecene	D-TiM41	3.1	83	9	70
•	G-TiM41	2.6	81	14	71
	D-TiNS	5.1	95	16	92
	G-TiNS	5.2	95	29	93
	TS-1	0.2	n.d.	n.d.	n.d.
2-Norbornene	D-TiM41	15	74	43	76
	G-TiM41	12	75	66	77
	D-TiNS	22	83	67	95
	G-TiNS	18	85	100	95
	TS-1	2.5	n.d.	n.d.	n.d.
1-Hexene	D-TiM41	1.2	55	3	75
	G-TiM41	1.0	50	5.5	75
	D-TiNS	12	95	37	95
	G-TiNS	3.5	75	19	94
	TS-1	20	95	55	95

^{*a*} Reaction conditions: catalyst, 35 mg; olefins, 12 mmol; H_2O_2 (35 wt%), 3.3 mmol; acetonitrile, 10 ml; 60 °C; reaction time, 2 h. ^{*b*} Conversion of olefins relative to the maximum possible (%). ^{*c*} Epoxide selectivity. ^{*d*} Moles of converted olefins per moles of Ti. ^{*e*} Oxidant efficiency = (amount used for olefin oxidation)/(amount used for olefin oxidation + amount decomposed) × 100 (%). Oxidant efficiency was evaluated by iodometric titration methods. ^{*f*} Not determined.

through direct synthesis. The G-TiM41 sample was prepared by post-synthetic Ti-grafting on MCM-41 silica. The D-TiNS sample was the 2.5 nm thick MFI zeolite nanosheets obtained with a titanosilicate composition by direct synthesis. TS-1 was a titanosilicate MFI zeolite with bulk crystal morphology. All the samples possessed Ti-sites mostly with a tetrahedral coordination, similar to G-TiNS (Fig. S4, ESI[†]).

In Table 2, the epoxidation catalytic performance of G-TiNS using H₂O₂ is presented in comparison with those of D-TiM41, G-TiM41, D-TiNS, and TS-1 catalysts for each reaction with cyclooctene, cyclododecene, 2-norbornene, and 1-hexene. In all the bulky molecular reactions, except for 1-hexene, the G-TiNS zeolite exhibited remarkably high olefin conversion and epoxidation selectivity, as compared to D-TiM41 and G-TiM41. Thus, the grafted Ti-sites on the zeolite nanosheets were more active than Ti-sites on the mesopore wall of MCM-41 amorphous titanosilicates. Another notable result was that G-TiNS possessed less Ti per weight than D-TiNS. Nevertheless, the grafted G-TiNS exhibited a catalytic conversion similar to that of D-TiNS in the bulky molecular reactions. This result is ascribed to Ti-sites located mostly on the external surface in D-TiNS. Comparatively, in the case of D-TiNS, the direct synthesis could incorporate a significant fraction of Ti into internal sites, as well as on the external surface. The internal Ti-sites would be inaccessible to bulky substrates due to the steric constraint of narrow micropore apertures. Following the same reasoning, the almost sole microporous TS-1 catalyst is believed to be almost inactive for the bulky molecular reactions.

G-TiNS exhibited higher epoxide selectivities (>95% with both cyclooctene and cyclododecene; 83% with 2-norbornene) than those of the MCM-41 titanosilicates (<83% with both cyclooctene and cyclododecene; <75% with 2-norbornene) for epoxidations of bulky olefins with H2O2. The selectivity difference between G-TiNS and MCM-41 can be attributed to the amorphous nature of the MCM-41 mesopore walls, and also to the high hydrophilic surface silanol concentration. We believe that the amorphous silicagrafted Ti species have a coordination that would deviate more from the perfect tetrahedral coordination than the crystalline zeolite-grafted Ti.²³ In addition, the weakly acidic silanol groups on MCM-41 could cause ring-opening reactions of the epoxide. It is also possible that the acidic silanols could cause decomposition of H₂O₂.^{13,23} Hence, the MCM-41 titanosilicates could exhibit lower H_2O_2 efficiency (<77%), as compared with those of G-TiNS (>93%). Compared to the MCM-41 catalysts, both the zeolite nanosheet catalysts (G-TiNS and D-TiNS) exhibited very high epoxide selectivity. This result indicated that the grafted Ti sites on the zeolite nanosheet could exhibit similar selectivity toward the external Ti sites in the zeolite framework for epoxidation of bulky olefins using H₂O₂.

For further characterization of the epoxidation ability of the G-TiNS catalyst, 1-hexene was tested as a substrate for epoxidation using H₂O₂. The bulk zeolitic TS-1 catalyst exhibited the best 1-hexene conversion (20%) and epoxidation selectivity (95%) (Table 2). The second best catalyst in this reaction was the directly synthesized zeolite nanosheet, i.e., D-TiNS. The D-TiNS catalyst exhibited a high epoxidation selectivity of 94%, but the conversion was only 12% (cf., 20% of TS-1). The high selectivity and low conversion can be explained if the epoxidation reaction of the highly hydrophobic 1-hexene could occur much more rapidly at the hydrophobic internal Ti-sites than the relatively hydrophilic external sites. As in our previous study on D-TiNS,²³ it is reasonable that the external silanols could be hydrated in the reaction environment using water. Hydration could increase the H₂O-coordination opportunity for neighboring Ti. This can also explain why the G-TiNS zeolite (possessing Ti sites mostly on the external surfaces) exhibited only 3.5% conversion with 75% selectivity. The selectivity could be increased to 85% by treatment with silylating agents or NH₄F. The details of the catalytic results and treatment are presented in the ESI.[†]

In summary, we demonstrated that post-synthetic Ti grafting onto 2.5 nm MFI zeolite nanosheets was a very simple and effective route to bulky olefin epoxidation catalysts using H_2O_2 . The epoxidation catalytic activity and selectivity of the resultant G-TiNS zeolite were much better than the corresponding properties of the MCM-41-type titanosilicates. In addition, the G-TiNS zeolite was recyclable for at least three cycles with a small decrease of conversion from 10.5% to 8.4% while maintaining its high selectivity (>94%). In contrast, G-TiM41 showed a serious decrease of conversion from 4.3% to 0.8% during the three cycles (Table S5, ESI†). The post-synthetic G-TiNS was similar to the directly synthesized D-TiNS when the epoxidation performance was compared as per Ti atom located on the external surfaces. Based on these results, post-synthetic Ti-grafting was believed to generate tetrahedral Ti-sites. We confirmed that external Ti grafting was also effective for the MFI zeolite nanosheets which were assembled into a nanosponge possessing uniform mesopore diameters.²⁹ Perhaps, other heteroatoms such as Sn, Zr, and V can be grafted in a similar manner onto the zeolite nanosponge. Post-synthetic grafting might generate suitable catalytic functions for other bulky molecular reactions.

This work was supported by IBS-R004-D1.

Notes and references

- 1 K. A. Jørgensen, Chem. Rev., 1989, 89, 431.
- 2 A. Corma and H. García, Chem. Rev., 2002, 102, 3837.
- 3 M. G. Clerice and P. Ingallina, J. Catal., 1993, 140, 71.
- 4 S. B. Kumar, S. P. Mirajkar, G. C. G. Pais, P. Kumar and R. Kumar, *J. Catal.*, 1995, **156**, 163.
- 5 S. C. Laha and R. Kumar, J. Catal., 2002, 208, 339.
- 6 P. Wu, T. Tatsumi, T. Komatsu and T. Yashima, *J. Catal.*, 2001, **202**, 245. 7 P. Wu, T. Tatsumi, T. Komatsu and T. Yashima, *J. Phys. Chem. B*,
- 2001, 105, 2897.
 8 S. Bordiga, F. Bonino, A. Damin and C. Lamberti, *Phys. Chem. Chem. Phys.*, 2007, 9, 4854.
- 9 E. Duprey, P. Beaunier, M.-A. Springuel-Huet, F. Bozon-Verduraz, J. Fraissard, J.-M. Manoli and J.-M. Brégeault, *J. Catal.*, 1997, **165**, 22.
- 10 T. Blasco, M. A. Camblor, A. Corma and J. Pérez-Pariente, J. Am. Chem. Soc., 1993, 115, 11806.

- 11 T. Blasco, A. Corma, M. T. Navarro and J. Pérez-Pariente, J. Catal., 1995, **156**, 65.
- 12 K. A. Koyano and T. Tatsumi, Chem. Commun., 1996, 145.
- 13 T. Tatsumi, K. A. Koyano and N. Igarashi, Chem. Commun., 1998, 325.
- 14 P. Wu and T. Tatsumi, Chem. Mater., 2002, 14, 1657.
- 15 G. D. Cremer, M. B. J. Roeffaers, E. Bartholomeeusen, K. Lin, P. Dedecker, P. P. Pescarmona, P. A. Jacobs, D. E. De Vos, J. Hofkens and B. F. Sels, *Angew. Chem., Int. Ed.*, 2010, **49**, 908.
- 16 F. Bérubé, B. Nohair, F. Kleitz and S. Kaliaguine, *Chem. Mater.*, 2010, 22, 1988.
- 17 L. Y. Chen, G. K. Chuah and S. Jaenicke, Catal. Lett., 1998, 50, 107.
- 18 J. Jarupatrakorn and T. D. Tilley, J. Am. Chem. Soc., 2002, 124, 8380.
- 19 A. Corma, U. Díaz, V. Fornés, J. L. Jordá, M. Domine and F. Rey, Chem. Commun., 1999, 779.
- 20 I. Schmidt, A. Krogh, K. Wienberg, A. Carlsson, M. Broson and C. J. H. Jacobsen, *Chem. Commun.*, 2000, 2157.
- 21 A. Corma, U. Diaz, M. E. Domine and V. Fornés, J. Am. Chem. Soc., 2000, 122, 2804.
- 22 P. Wu, D. Nuntasri, J. Ruan, Y. Liu, M. He, W. Fan, O. Terasaki and T. Tatsumi, *J. Phys. Chem. B*, 2004, **108**, 19126.
- 23 K. Na, C. Jo, J. Kim, W.-S. Ahn and R. Ryoo, ACS Catal., 2011, 1, 901.
- 24 X. Ouyang, S.-J. Hwang, D. Xie, T. M. Rea, S. I. Zones and A. Katz, *ACS Catal.*, 2015, 5, 3108.
- 25 C. B. Dartt and M. E. Davis, Appl. Catal., A, 1996, 143, 53.
- 26 P. Wu and T. Tatsumi, Chem. Commun., 2002, 1026.
- 27 J. Přech, D. Vitvarová, L. Lupínková, M. Kubů and J. Čejka, Microporous Mesoporous Mater., 2015, 212, 28.
- 28 K. Na, W. Park, Y. Seo and R. Ryoo, Chem. Mater., 2011, 23, 1273.
- 29 C. Jo, K. Cho, J. Kim and R. Ryoo, Chem. Commun., 2014, 50, 4175.